

Dissociation Dynamics and Stability of Cyclic Alkoxy Radicals and Alkoxide Anions

Leah S. Alconcel, Hans-Jürgen Deyerl, Michael DeClue, and Robert E. Continetti*

Contribution from the Department of Chemistry and Biochemistry, 0314, University of California, San Diego, 9500 Gilman Drive, La Jolla, California 92093-0314

Received December 14, 2000

Abstract: Photodetachment and dissociative photodetachment processes of cyclopropoxide, $c\text{-C}_3\text{H}_5\text{O}^-$, and cyclobutoxide have been studied at 532 nm. Photodetachment of $c\text{-C}_3\text{H}_5\text{O}^-$ produces both the ground $X(^2A')$ state and the first excited $A(^2A')$ state of cyclopropoxy radical, $c\text{-C}_3\text{H}_5\text{O}$. The $X(^2A')$ state is stable at lower levels of excitation, but with increasing internal energy, dissociation into $\text{HCO} + \text{C}_2\text{H}_4$ is observed. The $A(^2A')$ state completely dissociates into $\text{HCO} + \text{C}_2\text{H}_4$. Correlated measurements of photoelectron and photofragment kinetic energies provide dissociation energies $c\text{-C}_3\text{H}_5\text{O}^-$ and $c\text{-C}_3\text{H}_5\text{O}$ into $\text{HCO}^- + \text{C}_2\text{H}_4$ and $\text{HCO} + \text{C}_2\text{H}_4$ of 0.85 ± 0.07 and -0.26 ± 0.07 eV, respectively. Ab initio calculations have been performed to aid the interpretation of the dissociation mechanism. Cyclobutoxide, $c\text{-C}_4\text{H}_7\text{O}^-$, undergoes only dissociative photodetachment to ground-state vinoxy radical and ethylene. The adiabatic electron affinity (AEA) of $c\text{-C}_4\text{H}_7\text{O}$ is estimated to be 1.7 ± 0.1 eV. $c\text{-C}_4\text{H}_7\text{O}^-$ and $c\text{-C}_4\text{H}_7\text{O}$ are both found to be thermodynamically unstable relative to dissociation into $\text{C}_2\text{H}_3\text{O}^- + \text{C}_2\text{H}_4$ and $\text{C}_2\text{H}_3\text{O} + \text{C}_2\text{H}_4$ by -0.52 ± 0.07 and -0.45 ± 0.07 eV, respectively. Factors affecting the relative stability of the $c\text{-C}_3\text{H}_5\text{O}$ and $c\text{-C}_4\text{H}_7\text{O}$ radicals and the corresponding alkoxide anions are discussed on the basis of the observed differences in the dissociative photodetachment dynamics.

Introduction

Alkoxy radicals have been identified as important intermediates in atmospheric chemistry.¹ They are formed by reactions of volatile organic compounds with OH radicals and can react with O_2 to produce ketones and HO_2 , one of the catalysts for the formation of tropospheric ozone.^{1,2} The reactions of peroxy radicals with NO can also lead to the production of alkoxy radicals, which may subsequently react or undergo unimolecular dissociation to produce other reactive species.³ There has been considerable interest in developing an understanding of the reaction dynamics of these species.

The smallest cyclic alkoxy radicals are a particularly noteworthy case, because the geometric constraints in the cycloalkyl moiety force atypical bonding between the carbons. The bonding in cyclopropane and cyclobutane has been studied by theoretical and experimental methods.^{4–11} Despite the strain caused by the

60° bond angles between the carbons in the ring, the CC bond lengths in cyclopropane (1.51 Å)¹² are shorter than those of the n -alkanes (1.53 Å) and those of cyclobutane (1.55 Å).¹³ Cyclopropane undergoes reactions that are typical of CC double bonds and the HCH bond angle of 115.5° is also more consistent with the hybridization expected in unsaturated hydrocarbons. The angle strain in cyclobutane is lower, but torsional strain is higher since the CH bonds on neighboring carbons are not totally eclipsed. The ring strain energies of cyclopropane and cyclobutane are very similar as a consequence of these influences.^{7,14}

Coulson and Moffitt, through a quantum mechanical derivation, and Walsh, by deductions from empirical observations, demonstrated that the strain energy in cyclopropane is minimized if the bonds are not constrained to lie in the bond direction.^{15,16} Walsh proposed a model in which three sp^2 orbitals and one p orbital on each carbon are required to produce these “bent” bonds, resulting in localization of the CC bonding electron density outside or inside the ring. The bonding carbon sp^2 orbitals inside the ring are strongly overlapping, therefore that molecular orbital is low in energy. The carbon 2p orbitals outside the ring overlap to a lesser degree and produce two degenerate bonding molecular orbitals that are higher in energy. In the Coulson–Moffitt model, six sp^5 hybridized atomic orbitals on the carbons form three equivalent single bonds lying outside the ring. In contrast, the geometry of cyclobutane, including the $106.4^\circ \pm 1.3^\circ$ HCH angle,¹³ indicates that hybridization of the bonding atomic orbitals on the carbons in the ring is closer

- (1) Atkinson, R. *Int. J. Chem. Kinet.* **1997**, *29*, 99–111.
 (2) Jenkin, M. E.; Hayman, G. D. *Atmos. Environ.* **1999**, *33*, 1275–1293.
 (3) Poisson, N.; Kanakidou, M.; Crutzen, P. J. *J. Atmos. Chem.* **2000**, *36*, 157–230.
 (4) Pan, D.-K.; Gao, J.-N.; Lin, H.-L.; Huang, M.-B.; Schwartz, W. H. E. *Int. J. Quantum Chem.* **1986**, *29*, 1147–1154.
 (5) Hamilton, J. G.; Palke, W. E. *J. Am. Chem. Soc.* **1993**, *115*, 4159–4164.
 (6) Liu, B. L.; Kang, D. S. *J. Chem. Inform. Comput. Sci.* **1994**, *34*, 418–420.
 (7) Inagaki, S.; Ishitani, Y.; Kakefu, T. *J. Am. Chem. Soc.* **1994**, *116*, 5954–5958.
 (8) Karadakov, P. B.; Gerratt, J.; Cooper, D. L.; Raimondi, M. *J. Am. Chem. Soc.* **1994**, *116*, 7714–7721.
 (9) Karadakov, P. B.; Gerratt, J.; Cooper, D. L.; Raimondi, M. *Theochem-J. Mol. Struct.* **1995**, *341*, 13–24.
 (10) Allen, F. H.; Lommerse, J. P. M.; Hoy, V. J.; Howard, J. A. K.; Desiraju, G. R. *Acta Crystallogr. B-Struct. Sci.* **1996**, *52*, 734–745.
 (11) Zhao, C. Y.; Zhang, Y.; You, X. Z. *J. Phys. Chem. A* **1997**, *101*, 5174–5182.

- (12) Endo, Y.; Man Chai, C.; Hirota, E. *J. Mol. Spectrosc.* **1987**, *126*, 63–71.
 (13) Egawa, T.; Fukuyama, T.; Yamamoto, S.; Takabayashi, F.; Kambara, H.; Ueda, T.; Kuchitsu, K. *J. Chem. Phys.* **1987**, *86*, 6018–6026.
 (14) Cox, J. D.; Pilcher, G. *Thermochemistry of organic and organometallic compounds*; Academic Press: New York, 1970.
 (15) Coulson, C. A.; Moffitt, W. E. *Philos. Mag.* **1949**, *40*, 1–35.
 (16) Walsh, A. D. *Trans. Faraday Soc.* **1949**, *45*, 179–190.

to sp^3 . It is probable that the interaction of the molecular orbitals in the carbon ring with the 2p lone pairs on the oxygen atom strongly affects the chemistry of the cyclic alkoxy species.

The energetics of the low-lying states of the simplest cyclic alkoxy radical, cyclopropoxy, have been measured. Casey and Leopold obtained the negative-ion photodetachment spectrum of cyclopropoxide at 488 nm^{17,18} and determined the adiabatic electron affinity, 1.424 ± 0.006 eV for ground-state cyclopropoxy. The first excited state of cyclopropoxy was also observed and the excitation energy of the first excited state was measured to be 0.741 ± 0.002 eV. They suggested conjugation between the carbon 2p bonding orbitals in the ring and the out-of-plane oxygen 2p orbital stabilized the ${}^2A''$ ground state. The first excited state, ${}^2A'$, results from photodetachment from the in-plane oxygen lone pair. A Franck–Condon simulation of the photoelectron spectrum, assuming separable normal modes in the anion and neutral, was carried out with use of results from ab initio calculations with C_3 symmetry imposed. Contributions from isomeric anions, including acetone enolate, propionaldehyde enolate, and allyloxide, were observed as well. These species have similar electron affinities so vibronic transitions are observed in the same region of the photoelectron spectrum as the cyclopropoxy vibronic transitions. Broadening of the vibronic features in the ${}^2A'$ state was observed and attributed to a rapid opening of the cyclopropoxy radical ring to form the more stable 3-oxopropan-1-yl radical.

In this study, photodetachment of cyclopropoxide to the $X({}^2A'')$ and $A({}^2A')$ states of the stable neutral radical and dissociative photodetachment of both states to formyl radical and ethylene were observed at 532 nm. To aid in the interpretation of the experimental results, ab initio calculations have been carried out on cyclopropoxide and the ground and first excited states of the cyclopropoxy radical. The energetics and geometries of the species involved in the most probable dissociation mechanism, ring opening followed by C–C bond fission, were calculated and compared to experimental values and observations. Photodetachment of cyclobutoxide resulted only in dissociation to the ground state of the vinoxy radical, $X({}^2A'')$, and ethylene at 532 nm. There are no previous spectroscopic or thermodynamic data available for cyclobutoxide.

Experimental Section

The fast-ion-beam photoelectron–photofragment coincidence spectrometer used in these experiments has previously been described in detail.¹⁹ Recently, the photoelectron detector has been modified to include a space-focusing assembly implemented by Hayden and co-workers that permits the collection of 4πsr of photodetached electrons, in contrast to the 4% fraction collected via straight time-of-flight.²⁰ A potential applied to the repeller plate accelerates the electrons toward a time- and position-sensitive detector. Energy and angular distributions can be extracted from the 2D images and time information obtained.

Cyclopropanol was synthesized according to procedures developed previously.^{21–23} It was purified (90–95%) by gas chromatography. Either cyclopropanol cooled to -10 °C or spectro-grade cyclobutanol (Acros, 99+%) at room temperature was seeded in a 10% mixture of N_2O in Ar and produced anions in a pulsed discharge ion source.²⁴

The anions were accelerated to 3 keV and the mass-selected beam at m/e 57 or 71 was intersected by the linearly polarized second harmonic (532 nm, 2.33 eV) of a Nd:YAG laser.

The photodetached electrons are accelerated by a small potential (ca. 1.5 V/mm) over a distance of 6 mm and pass through a grid into a 12 mm field-free flight region. After passing through a final grid, the electrons are accelerated onto a 40-mm diameter time- and position-sensitive detector in a single-field space-focusing time-of-flight (TOF) arrangement. During analysis, the x - and y -velocity components of the photoelectron in the center-of-mass (CM) frame are determined relative to the center of the observed two-dimensional image rather than the center of the detector to correct for the Doppler shift caused by the fast ion beam. The z -velocity component is determined by TOF, and is the limiting factor in the energy resolution using the 100 ps pulse width Nd:YAG laser in this study. From this direct determination of the three-dimensional recoil velocity of the photoelectron, the electron kinetic energy (eKE) in the center-of-mass (CM) frame is calculated. The overall resolution in eKE is $\sim 12\%$ $\Delta E/E$, determined from calibration with O^- ; however, selecting photoelectrons with minimal z -velocity components yields higher resolution ($\sim 8\%$ $\Delta E/E$ in O^-). Photoelectron spectra for cyclopropoxide were recorded in coincidence with stable m/e 57 and with $HCO + C_2H_4$ photofragments. For cyclobutoxide, only dissociation was observed and the photoelectrons were recorded in coincidence with the $C_2H_3O + C_2H_4$ photofragments.

The neutral photofragments from the dissociation of the cyclopropoxy and cyclobutoxy radicals were detected by the photofragment translational spectrometer. The fragments recoil out of the beam over a 96 cm flight path and, if they clear a 7 mm wide horizontal beam block, impinge upon a time- and position-sensitive detector. An electrostatic deflector removes residual anions from the beam. Conservation of linear momentum between the photofragment pairs in the CM frame is used to ensure that the fragments originated from a single dissociation event and to determine the fragment masses. The mass resolution is limited to $m/\Delta m < 15$,²⁵ thereby precluding definitive assignment of the product masses from the spectrum alone. Energetics and structure are also considered to determine the most plausible fragmentation pathway. The dissociation of cyclopropoxy into formyl radical and ethylene includes the formation of a stable unsaturated hydrocarbon and the simple fission of two C–C bonds, therefore it is deemed favorable over other channels that require hydrogen shifts. The dissociation of cyclobutoxy into vinoxy radical and ethylene is considered to be favorable for the same reasons. Once the product masses are assigned, the center-of-mass translational energy release, E_T , is calculated. Contributions from false coincidences are estimated to be $\approx 6\%$.²⁶

Calculations

Ab initio calculations were carried out with the Gaussian 98 program suite²⁷ on the Cray T90 supercomputer located at the San Diego Supercomputer Center. The ab initio results were used to assist in the interpretation of features in the stable cyclopropoxide photoelectron spectrum and to follow the most facile reaction path to dissociation of the cyclopropoxy radical. Single reference wave function geometry optimizations and

(25) Continetti, R. E. In *Photoionization and Photodetachment*; Ng, C. Y., Ed.; World Scientific: Singapore, 2000; Vol. 10B, pp 748–808.

(26) Continetti, R. E. *Int. Rev. Phys. Chem.* **1998**, *17*, 227–260.

(27) Frisch, M. J.; Trucks, G. W.; Schlegel, H. B.; Scuseria, G. E.; Robb, M. A.; Cheeseman, J. R.; Zakrzewski, V. G.; Montgomery, J. J. A.; Stratmann, R. E.; Burant, J. C.; Dapprich, S.; Millam, J. M.; Daniels, A. D.; Kudin, K. N.; Strain, M. C.; Farkas, O.; Tomasi, J.; Barone, V.; Cossi, M.; Cammi, R.; Mennucci, B.; Pomelli, C.; Adamo, C.; Clifford, S.; Ochterski, J.; Petersson, G. A.; Ayala, P. Y.; Cui, Q.; Morokuma, K.; Malick, D. K.; Rabuck, A. D.; Raghavachari, K.; Foresman, J. B.; Cioslowski, J.; Ortiz, J. V.; Baboul, A. G.; Stefanov, B. B.; Liu, G.; Liashenko, A.; Piskorz, P.; Komaromi, I.; Gomperts, R.; Martin, R. L.; Fox, D. J.; Keith, T.; Al-Laham, M. A.; Peng, C. Y.; Nanayakkara, A.; Gonzalez, C.; Challacombe, M.; Gill, P. M. W.; Johnson, B.; Chen, W.; Wong, M. W.; Andres, J. L.; Gonzalez, C.; Head-Gordon, M.; Replogle, E. S.; Pople, J. A. *Gaussian 98*, Revision A.7; Gaussian, Inc.: Pittsburgh, 1998.

(17) Casey, S. M. Ph.D. Thesis, University of Minnesota, 1993.

(18) Casey, S. M.; Leopold, D. G. Unpublished work.

(19) Hanold, K. A.; Continetti, R. E. *Chem. Phys.* **1998**, *239*, 493–509.

(20) Davies, J. A.; LeClaire, J. E.; Continetti, R. E.; Hayden, C. C. *J. Chem. Phys.* **1999**, *111*, 1–4.

(21) Ruehlmann, K. *Synthesis* **1971**, 236–253.

(22) Salauen, J. *J. Org. Chem.* **1976**, *41*, 1237–1240.

(23) Salauen, J.; Bennani, F.; Compain, J.-C.; Fadel, A.; Ollivier, J. J. *Org. Chem.* **1980**, *45*, 4129–4135.

(24) Zengin, V.; Persson, B. J.; Strong, K. M.; Continetti, R. E. *J. Chem. Phys.* **1996**, *105*, 9740–9747.

frequency calculations at the MP2²⁸ level of theory were carried out on the ground-state species studied, with the exception of the transition state between cyclopropoxide and 3-oxopropan-1-ide. A single-point MP2 calculation was performed on the optimized HF geometry of this species and it is evident from the energetics that the optimized MP2 structure would not differ significantly. The excited-state optimizations and frequency calculations were performed with the configuration interaction method including single excitations (CIS).^{29,30} Multireference wave function calculations were deemed beyond the scope of this study, since the cost of including all of the CC bonding and antibonding orbitals and the O 2p and 2p' orbitals in the active space would be prohibitive. To confirm that the reaction path between minima passed through the calculated transition states, intrinsic reaction coordinate (IRC) calculations were performed.³¹ The Pople valence triple- ζ basis set³² including diffuse and polarization functions on the heavy atoms (6-311+G*) was used. The diffuse functions are required to more accurately compute the absolute energy of the anionic species. The energetics were refined with single-point QCISD³³ calculations that are bound by the exact solution to the wave function, since the perturbative energies are not.

Results

Cyclopropoxide undergoes photodetachment to both the ground and first excited states of the cyclopropoxy radical at 532 nm. An image of the photoelectrons obtained from all detachment events was obtained by removing the beam block and requiring coincidence with one neutral product (Figure 1a). The image of the photoelectrons resulting from dissociative photodetachment that is shown in Figure 1b required coincident detection with a pair of neutral photofragments. The electron angular distribution is nearly isotropic, as evidenced by the similarity of the images obtained with the electric vector of the laser parallel or perpendicular to the face of the electron detector. The most striking feature in these images is the intense peak at the center, resulting primarily from very low energy photoelectrons which could not have been detected previously by using the straight time-of-flight photoelectron detector on this apparatus.

Photoelectron spectra of cyclopropoxide are shown in Figure 2. Spectrum a shows photoelectrons recorded in coincidence with at least one photofragment. Spectrum b shows photoelectrons recorded in coincidence with stable neutral products, identified as the single photofragments that impinged upon the heavy particle detector at the beam velocity. In spectrum c, the signal from the photoelectrons recorded in coincidence with two dissociative photofragments is shown. The three regions of interest in the photoelectron spectra consist of a broad, low-intensity feature at high eKE corresponding to stable neutral radicals, a feature peaking at ~ 0.6 eV corresponding to both stable radicals and dissociative fragments, and two peaks at low eKE corresponding only to dissociative fragments. These peaks are emphasized in the dashed curve in spectrum c, which shows only those photoelectrons with minimal velocity components perpendicular to the face of the detector.

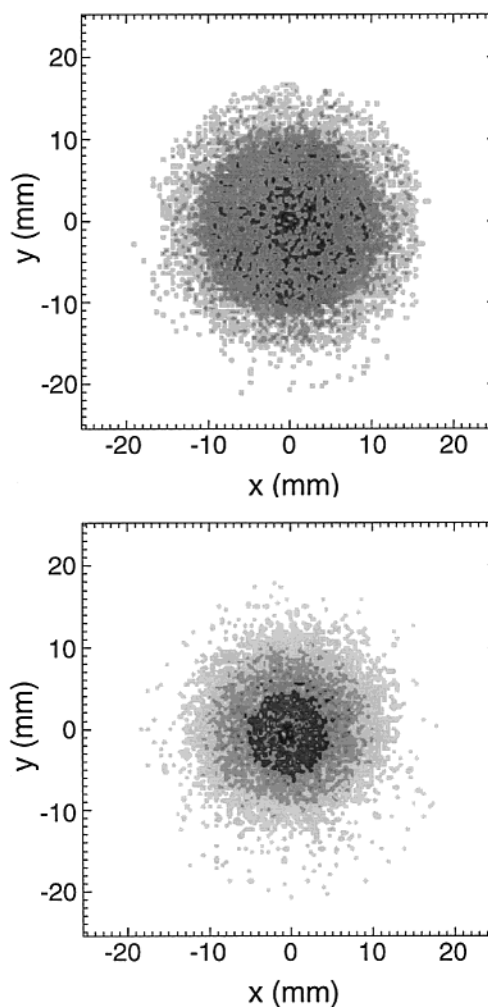


Figure 1. Photoelectron images of cyclopropoxide. Image of electrons detected in coincidence (a) with at least one neutral fragment, stable or dissociative, and (b) with two dissociative photofragments. The laser polarization is perpendicular to the face of the photoelectron detector in part a. The data shown in part b include both parallel and perpendicular polarizations since the photoelectron angular distribution is isotropic.

The photoelectron–photofragment kinetic energy correlation spectra of both cyclopropoxide and cyclobutoxide at 532 nm are displayed as contour maps in Figure 3. These spectra show how the available kinetic energy is partitioned between the photoelectron and the photofragments for the dissociation processes observed. The y-axis is the photoelectron spectrum, $N(eKE)$, and the x-axis is the photofragment translation energy released spectrum, $N(E_T)$. At higher levels of excitation the $X(^2A'')$ state of c-C₃H₅O dissociates, and the $A(^2A')$ state is found to be entirely dissociative (Figure 3a). The $N(E_T)$ distribution from the dissociation of cyclopropoxy is observed to peak at 0.26 ± 0.05 eV. Figure 3b shows that in the dissociative photodetachment of the $X(^2A'')$ state of cyclobutoxy, the $N(E_T)$ peaks at 0.30 ± 0.05 eV.

Discussion

The features in the cyclopropoxide photoelectron images and spectra are analyzed and compared to previous experimental results in section A. In section B, the dissociation energies of the cyclopropoxy and cyclobutoxy radicals and the corresponding alkoxide anions are determined from the correlation spectra. Factors affecting the relative stabilities of these species are

(28) Moller, C.; Plesset, M. S. *Phys. Rev.* **1934**, *46*, 618–622.

(29) Foresman, J. B.; Head-Gordon, M.; Pople, J. A.; Frisch, M. J. *J. Phys. Chem.* **1992**, *96*, 135–149.

(30) Trucks, G. W.; Frisch, M. J. To be submitted for publication.

(31) Gonzalez, C.; Schlegel, H. B. *J. Chem. Phys.* **1989**, *90*, 2154–2161.

(32) Krishnan, R.; Binkley, J. S.; Seeger, R.; Pople, J. A. *J. Chem. Phys.* **1980**, *72*, 650–654.

(33) Pople, J. A.; Head-Gordon, M.; Raghavachari, K. *J. Chem. Phys.* **1987**, *87*, 5968–5975.

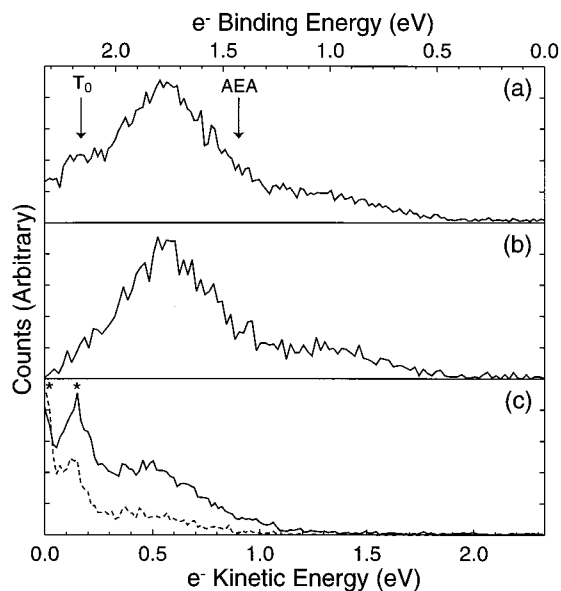


Figure 2. Photoelectron spectra of cyclopropoxide. The spectra of (a) stable and dissociative events, (b) stable events, and (c) dissociative events are shown. Additionally, the dashed curve in frame c shows photoelectrons with minimal velocity components perpendicular to the detector plane, emphasizing the near-ZEKE photoelectrons and revealing more clearly the vibronic structure (marked with asterisks) observed in the $A(^2A')$ state of the cyclopropoxy radical.

discussed. Finally, a comparison of the experimental and ab initio energies for the species involved in cyclopropoxide photodetachment and the dissociation of the cyclopropoxy radical is presented in section C.

A. Photoelectron Images and Spectra. For the cyclopropoxy radical, there are three energetic regions of interest present in the photoelectron images and spectra. The first occurs in the range of eKEs between 1.05 and 1.85 eV and is composed of photoelectrons coincident with a stable neutral product. The second region is in the range of 0.20 to 1.05 eV and has contributions from photoelectrons coincident with both stable radicals and dissociation products. The stable component of the spectrum peaks at about 0.60 eV and the dissociative component at about 0.50 eV. The photoelectrons with energies from 0 to 0.20 eV comprise the third region, corresponding to dissociation. In this region, vibrational structure is observed in the dissociative photoelectron spectrum c with peaks at 0 and 0.14 eV that are marked with asterisks.

The broad, low-intensity feature at high eKE in the stable photoelectron spectrum has previously been attributed to photodetachment from an isomeric carbanion form of cyclopropoxide.¹⁷ Since no resolved vibrational transitions were observed in this portion of the spectrum in the present study or previously by Casey, the anion could not be unambiguously identified. The low electron affinity and the absence of a contribution from this anion to the dissociative photoelectron spectrum indicate that photodetachment of 3-oxopropan-1-ide, the ring-opened carbanion form of cyclopropoxide, may give rise to this feature. The 3-oxopropan-1-yl neutral radical that is formed by photodetachment of this species is the same radical that is formed in the proposed ring-opening dissociation mechanism of cyclopropoxy. According to the dissociation mechanism, 3-oxopropan-1-yl subsequently undergoes carbon-carbon bond fission to produce formyl radical and ethylene. However, it is possible that 3-oxopropan-1-yl produced by photodetachment of the cold anion is stable, while that produced by opening the

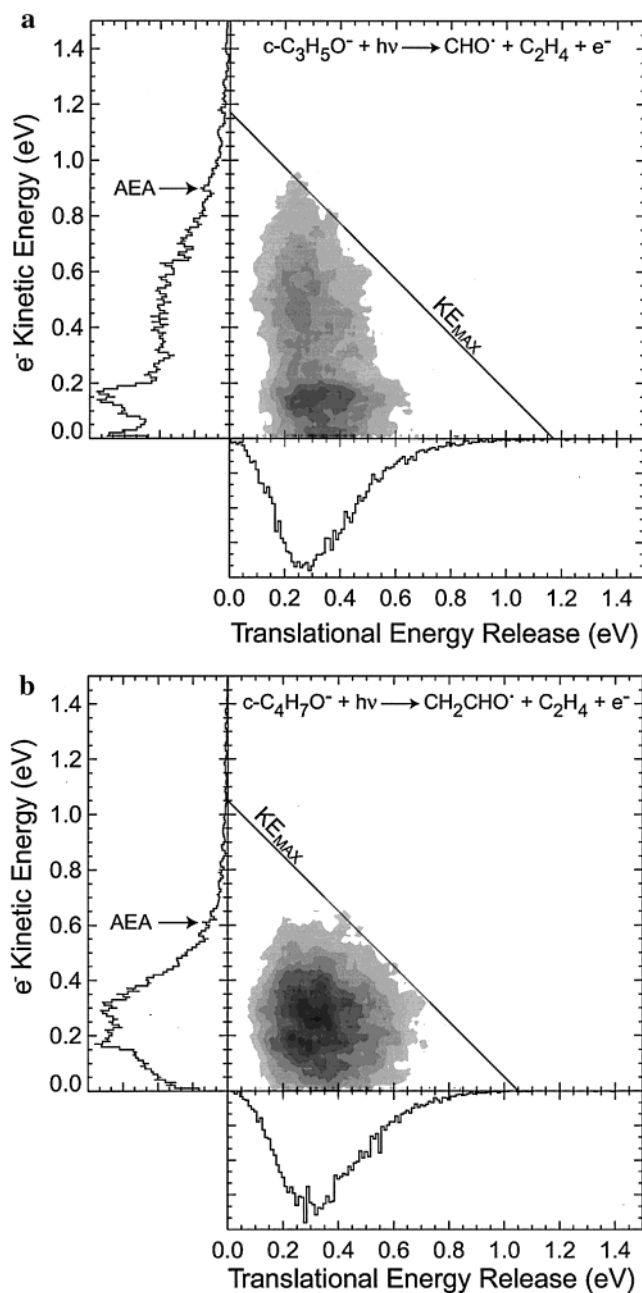


Figure 3. Photoelectron-photofragment kinetic energy correlation spectra ($N(E_T, eKE)$) of cyclopropoxide (a) and cyclobutoxide (b). The photoelectron spectrum ($N(eKE)$) is shown on the y-axis and the photofragment translational energy spectrum ($N(E_T)$) is shown on the x-axis. These one-dimensional spectra are obtained by integration of the correlation spectrum over the conjugate variable.

cyclopropoxy ring has the energy required to undergo rapid dissociation.

An analysis of the ab initio structures and frequencies yields insight into the spectral features. The bond lengths and angles obtained from geometry optimizations with the MP2 or CIS method and the 6-311+G* basis set for cyclopropoxide and the $X(^2A')$ and $A(^2A')$ states of the neutral cyclopropoxy radical are shown in Table 1. No experimentally determined structural parameters are available for these species. The atom labeling is shown in Figure 4. Cyclopropoxide and the cyclopropoxy radicals have a plane of symmetry defined by the OC_1H_1 bond angle. The results from the normal mode calculations, with frequencies scaled by 0.92, are compared with experimental frequencies in Table 2.³⁴ The bending and stretching modes that

Table 1. Structures of Species Involved in Cyclopropoxide Photodetachment^a

species	C ₁ -C ₂	C ₂ -C ₃	C ₁ -C ₃	C ₁ -O	∠C ₂ C ₁ C ₃	∠C ₁ C ₂ C ₃	∠OC ₁ H ₁
cyclopropoxide	1.543	1.530	1.543	1.322	59.4	60.3	118.3
anion T.S.	1.472	1.520	1.968	1.238	49.9	82.2	119.9
3-oxopropan-1-ide	1.485	1.527	2.315	1.247		100.5	119.6
cyclopropoxy (X)	1.593	1.458	1.593	1.271	54.5	62.8	121.4
radical T.S. 1	1.549	1.456	1.766	1.236	51.6	71.9	122.6
3-oxopropan-1-yl	1.521	1.496	2.467	1.215		109.7	120.4
radical T.S. 2	2.152	1.351	2.837	1.182		105.9	125.2
formyl + ethene		1.339		1.184			123.6
cyclopropoxy (A)	1.482	1.524	1.482	1.384	61.9	59.1	108.7
radical T.S. 3	1.483	1.482	2.024	1.399	46.9	86.1	113.6

^a Calculated with the MP2 or CIS methods and the 6-311+G* basis set. Atom labels are in Figure 4; bond lengths are given in angstroms and angles in degrees

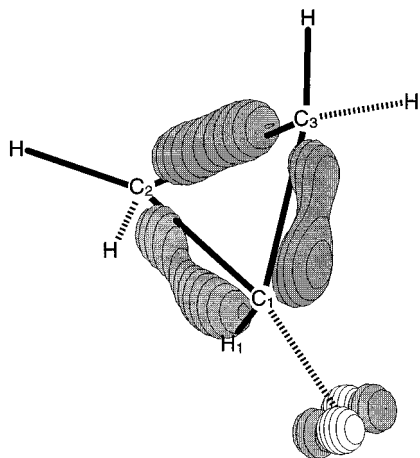


Figure 4. Cyclopropoxy structure and molecular orbitals. The plane of symmetry is defined by the OC₁H₁ bond angle. The ring and a'' O σ_{2p} orbitals are shown in gray. The a' O σ_{2p} orbital is shown in white. The atom labels given are used in Table 1 and in the text. This figure was generated using MOLDEEN (Schaftenaar, G.; Noordik, J. H. J. *Comput.-Aided Mol. Design* **2000**, *14*, 123–134).

are symmetric about or confined to the plane are designated as a' and those that are asymmetric with respect to the plane are designated as a''. The modes have been ordered ν₁–ν₂₁ according to the results for the X(2A'') state of the cyclopropoxy radical and designated by the dominant atomic displacements. The same mode descriptions are applicable to the results for the anion and the A(2A') state of the cyclopropoxy radical and the frequencies for these species have been arranged correspondingly. The major geometry changes from the anion to the ground-state neutral radical are in the CC bond lengths and CCC bond angles in the cyclopropyl moiety. From the anion to the first excited state neutral radical, the largest geometry change is in the OC₁H₁ bond angle. The dominant displacements in the normal modes that give rise to the most intense transitions in the photoelectron spectra as identified by Casey¹⁷ correspond to these geometry changes.

In the region of the photoelectron spectrum corresponding to X(2A'') ← X(1A') photodetachment, the lack of vibrational resolution made the assignment of observed spectral features difficult. Therefore, a detailed analysis is not presented here. In general, the low-resolution experimental photoelectron spectrum reported here is in agreement with the previous experimental results. The contributions which Casey observed from geometric isomers such as *n*-propionaldehyde enolate (AEA = 1.6175 ± 0.0087 eV)³⁵ and acetone enolate (AEA =

Table 2. Scaled Frequencies (see text) of Normal Vibrational Modes (in cm⁻¹) for Cyclopropoxide and the Cyclopropoxy Radicals^a

vibration	X(1A')		X(2A'')		A(2A')	
	theor	exp ^b	theor	exp ^b	theor	exp ^b
ν ₁ , CH ₂ antisym str, a'	2970		3050		3103	
ν ₂ , CH ₂ sym str, a'	2860		2939		3020	
ν ₃ , CH str, a'	2612		2861		3043	
ν ₄ , CH ₂ sym bend, a'	1369		1403		1526	
ν ₅ , CH i.p. bend, a'	1281		1276		1389	1265
ν ₆ , CO str, a'	1164		1230		1121	
ν ₇ , ring breathing, a'	1072		1127	1155	1218	
ν ₈ , CH ₂ sym wag, a'	897	970	966	955	1074	
ν ₉ , ring deformation, a'	948		870	700	976	
ν ₁₀ , CH ₂ twist, a'	750		753		791	
ν ₁₁ , CH ₂ rock, a'	697		608		739	
ν ₁₂ , CO deformation, a'	385	385	396	450	377	
ν ₁₃ , CH ₂ sym str, a''	2953		3036		3088	
ν ₁₄ , CH ₂ antisym str, a''	2849		2934		3015	
ν ₁₅ , CH ₂ antisym bend, a''	1339		1361		1465	
ν ₁₆ , CH ₂ twist, a''	1107		1134		1209	
ν ₁₇ , CH o.o.p. bend, a''	1028		994		1139	
ν ₁₈ , CH ₂ antisym wag, a''	891		958		1110	
ν ₁₉ , CO o.o.p. bend, a''	786		757		1024	
ν ₂₀ , ring deformation, a''	591		459		818	
ν ₂₁ , CO deformation, a''	385		276		419	

^a Calculated with MP2 or CIS methods and the 6-311+G* basis set. a' and a'' indicate the C_s symmetry of the vibrational modes. In-plane (i.p.) and out-of-plane (o.o.p.) modes are specified. Available experimental parameters are provided. ^b Reference 17.

1.757 ± 0.033 eV)³⁶ in this energetic region could not have been distinguished in this spectrum.¹⁷ However, it is unlikely that the anion source in this experiment produced significant amounts of the isomeric enolates of cyclopropoxide or cyclobutoxide. Photodetachment studies at 355 nm of *n*-propionaldehyde and acetone enolates as well as the *n*-, *sec*- and isobutyraldehyde enolates have been performed in this laboratory and all species are stable following photodetachment at 3.494 eV.³⁷ If the isomeric enolates of cyclobutoxide had been present in the ion beam, the cyclobutoxide data would have contained a stable component that was not observed. Hence, it is also improbable that the isomeric enolates of cyclopropoxide were formed in the source; however, the presence of some of these species in the stable radical component observed in the X(2A'') region of the photoelectron spectrum cannot be ruled out.

In the A(2A') ← X(1A') transition observed at low eKE in the dissociative photoelectron spectrum of c-C₃H₅O⁻, significant excitation occurs in a single vibrational mode, ν₅, corresponding to the CH in-plane bend (Table 2). The resolution of the two vibrational peaks is accentuated when only photoelectrons with

(34) Scott, A. P.; Radom, L. *J. Phys. Chem.* **1996**, *100*, 16502–16513.
 (35) Romer, B. C.; Brauman, J. I. *J. Am. Chem. Soc.* **1997**, *119*, 2054–2055.

(36) Ellison, G. B.; Engelking, P. C.; Lineberger, W. C. *J. Phys. Chem.* **1982**, *86*, 4873–4878.

(37) Alconcel, L. S.; Continetti, R. E. To be submitted for publication.

minimal velocity components perpendicular to the face of the detector are considered, as shown by the dashed curve in Figure 2c. Excitation of the $\nu' = 1$ state of the ν_5 mode is the most likely explanation for the peak observed at zero electron kinetic energy (ZEKE) in the correlation spectrum. It is reasonable that ν_5 would be active, since the major geometrical change from cyclopropoxide to the $A(^2A')$ state of the cyclopropoxy radical is contraction of the OC_1H_1 bond angle by nearly 10° (Table 1). Upon dissociation into formyl and ethylene, the OC_1H_1 bond angle expands by 15° . Casey found significant Franck–Condon overlap only in ν_5 . He measured the peak spacing between the 0–0 transition from the anion to the first excited state and the $\nu' = 1$ transition in ν_5 to be $1265 \pm 15 \text{ cm}^{-1}$ in the stable photoelectron spectrum. The peak spacing between the 0–0 transition from the anion to the first excited state and the ZEKE peak in the current study is $1129 \pm 160 \text{ cm}^{-1}$. A significant cross-section for photodetachment at threshold implies that the electron is detached with no angular momentum in an s-wave. According to the algorithm developed by Brauman and co-workers for determining the photodetachment cross section near threshold, s-wave photodetachment from the a' symmetry HOMO–1 of cyclopropoxide should be allowed.³⁸ The observation of the ZEKE peak is thus consistent with s-wave photodetachment from a p-like orbital, specifically the in-plane (a') oxygen σ_{2p} orbital in this case.

B. $N(E_T, eKE)$ Correlation Spectra. The dissociative photodetachment events plotted in Figure 3 are constrained by conservation of energy to lie within the triangle formed by the x - and y -axes and the maximum available kinetic energy, KE_{MAX} . The diagonal line drawn at the 5% contour in Figure 3a provides an estimate of $KE_{MAX} = 1.17 \pm 0.07 \text{ eV}$. This value of KE_{MAX} can be used to determine the energetics of the anionic and neutral system with the assumptions that photodetachment of vibrationally cold anions occurs, and in the dissociation process some fragments are produced with no internal energy. By using the photon energy, KE_{MAX} , and the electron affinity of HCO ($0.3130 \pm 0.0050 \text{ eV}$),³⁹ the dissociation energy of cyclopropoxide relative to the formyl anion and ethylene, $D_0(c\text{-}C_3H_5O^-)$, is found to be $0.85 \pm 0.07 \text{ eV}$. Substitution of the electron affinity of cyclopropoxy in the same calculation yields the dissociation energy of cyclopropoxy relative to formyl radical and ethylene, $D_0(c\text{-}C_3H_5O) = -0.26 \pm 0.07 \text{ eV}$. The experimental energetics are shown in Figure 5a. The correlation spectrum also demonstrates that the lifetime broadening in the $A(^2A')$ state that Casey attributed solely to ring-opening of the excited cyclopropoxy radical in fact results from ring-opening followed by dissociation. The vibrational structure observed in the dissociative photoelectron spectrum shows that the $A(^2A')$ state cyclopropoxy radical lifetime, though shorter than the flight time ($\sim 10 \mu\text{s}$), is longer than the period of the ν_5 vibration ($\sim 100 \text{ fs}$).

The occurrence of photodetachment to a stable as well as a dissociative component of the $X(^2A'')$ state of the cyclopropoxy radical indicates, by extension of the Coulson–Moffitt and Walsh models for bonding in cyclopropane, that the singly occupied a'' oxygen σ_{2p} orbital conjugates with the bent bonds lying outside the cyclopropyl ring. The interaction of these orbitals, illustrated in gray in Figure 4, results in stabilization of the radical. The singly occupied a' oxygen σ_{2p} orbital, shown in white in Figure 4, would not be expected to interact with the bonds lying outside the carbon ring, yielding a less stable

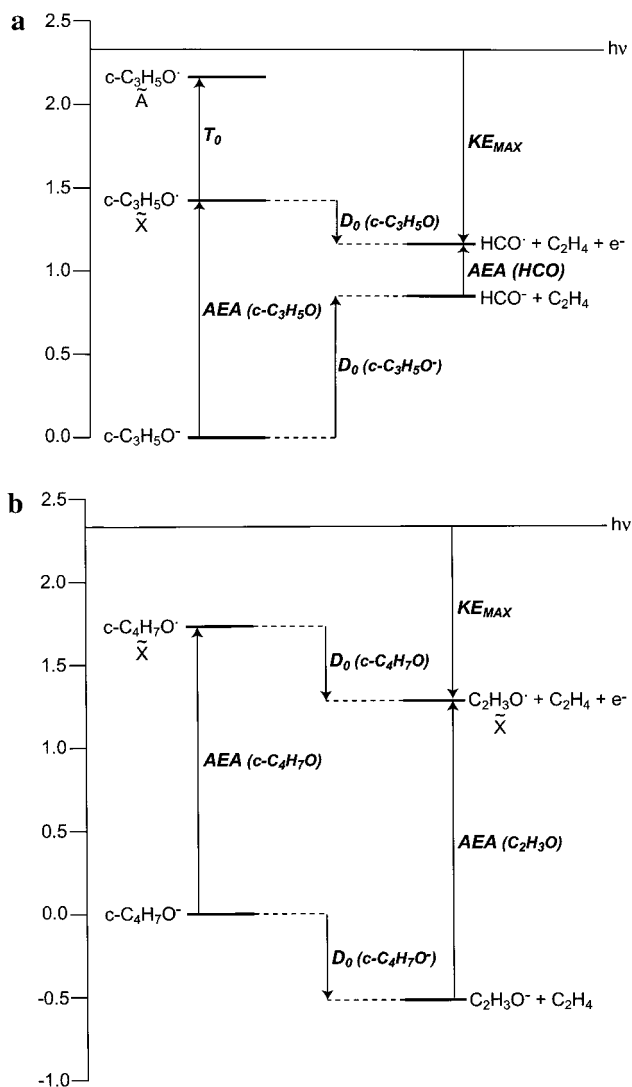


Figure 5. Potential energy diagrams (energies in eV) for the species involved in cyclopropoxide (a) and cyclobutoxide (b) photodetachment. Energy differences are from Table 4 and as discussed in the text.

configuration in the $A(^2A')$ state and the prompt dissociation that has been observed in this study. These electronic configurations resemble those of the $X(^2A'')$ and $A(^2A')$ states of the vinoxy radical. In the ground state of the vinoxy radical, the singly occupied a'' oxygen σ_{2p} orbital conjugates with the π orbitals on the carbons, while the singly occupied a' oxygen σ_{2p} orbital of the first excited state does not. The similarity in magnitude of the splitting between $X(^2A'')$ and $A(^2A')$ states (0.741 eV)¹⁷ in cyclopropoxy to the splitting between the $X(^2A'')$ and $A(^2A')$ states (1.015 eV)⁴⁰ of the vinoxy radical supports this comparison of the molecular orbital configurations.

The $N(E_T)$ distribution in the dissociation of the cyclobutoxy radical shown in Figure 3b peaks at a higher value, $0.30 \pm 0.05 \text{ eV}$, indicating either greater repulsion between the neutral fragments or less partitioning of the available energy to internal degrees of freedom compared to cyclopropoxy. The latter explanation is not likely due to the greater density of states of the products of the dissociation of cyclobutoxy. The electron affinity of the cyclobutoxy radical is estimated from this spectrum to be $1.7 \pm 0.1 \text{ eV}$. The diagonal line drawn at the 5% contour provides an estimate of KE_{MAX} of $1.05 \pm 0.07 \text{ eV}$

(38) Reed, K. J.; Zimmerman, A. H.; Andersen, H. C.; Brauman, J. I. *J. Chem. Phys.* **1976**, *64*, 1368–1375.

(39) Murray, K. K.; Miller, T. M.; Leopold, D. G.; Lineberger, W. C. *J. Chem. Phys.* **1986**, *84*, 2520–2525.

(40) Alconcel, L. S.; Deyerl, H. J.; Zengin, V.; Continetti, R. E. *J. Phys. Chem. A* **1999**, *103*, 9190–9194.

Table 3. Absolute Energies, Corrected by Zero Point Energies, in Hartrees, for the Species Involved in Cyclopropoxide Photodetachment

	species	HF/6-311+G*	MP2/6-311+G*	QCISD/6-311+G*
1	cyclopropoxide	-191.2624427	-191.8940201	-191.9220142
2	anion T.S.	-191.2457896	-191.8769301	-191.9039499
3	3-oxopropan-1-ide	-191.2534037	-191.8836930	-191.9122453
4	cyclopropoxy (X)	-191.2718314	-191.8465377	-191.8842616
5	radical T.S. 1	-191.2723552	-191.8502926	-191.8825545
6	3-oxopropan-1-yl	-191.2956972	-191.8715463	-191.9066509
7	radical T.S. 2	-191.2599073	-191.8320803	-191.8636700
8	formyl + ethene	-191.2663243	-191.8463710	-191.8823246
9	cyclopropoxy (A)	-191.2632072	-191.8264060	-191.8683558
10	radical T.S. 3	-191.2652873	-191.8222459	-191.8606025

that can be used to determine the energetics of this system with the conditions mentioned above in the discussion of cyclopropoxide. Given KE_{MAX} , the photon energy, and the electron affinities of cyclobutoxy and vinoxy (1.795 ± 0.015 eV),⁴⁰ the dissociation energies of cyclobutoxy and cyclobutoxy radical relative to ethylene and vinoxy or vinoxy radical were determined. These are shown in Figure 5b, where $D_0(c-C_4H_7O^-)$ is -0.52 ± 0.07 eV and $D_0(c-C_4H_7O)$ is -0.45 ± 0.07 eV, showing that both the anionic and neutral species are energetically unstable relative to these dissociation pathways. It cannot be directly determined whether photodetachment occurs from cyclobutoxy or the ring-opened carbanion, 4-oxobutan-1-ide. However, the cyclopropoxide data suggest that photodetachment from the ring-opened carbanion does not lead to prompt dissociation of the resulting radical. Several theoretical studies have shown that the thermal cycloaddition of two ethylenes to form cyclobutane proceeds stepwise via ring-opening to the tetramethylene biradical, since the concerted cycloaddition is forbidden by the Woodward–Hoffmann rules for pericyclic reactions.^{41–44} A stepwise dissociation of cyclobutoxy through a ring-opened radical is therefore deemed most probable.

Dissociation into ethylene and ground $X(^2A'')$ state vinoxy indicates that the electron is photodetached from the a'' oxygen σ_{2p} orbital. The prompt dissociation suggests that conjugation with the molecular orbitals in the carbon ring does not stabilize the cyclobutoxy radical as much as the cyclopropoxy radical ground state. Thermal cycloaddition of the products would occur via an antarafacial, or geometrically unfavorable, transition state according to the symmetries of the CCO π^* LUMO of ground-state vinoxy and the HOMO of ethylene.⁴¹ This may also increase the reactivity of the cyclobutoxy radical relative to the cyclopropoxy radical. The electronic configuration of the cyclobutoxy radical is similar to that of the ethoxy radical, in which the singly occupied a'' and a' oxygen σ_{2p} orbitals of the $X(^2A'')$ and $A(^2A')$ states do not conjugate with the ethyl moiety. The splitting between the $X(^2A'')$ and $A(^2A')$ states in ethoxy is very small (355 ± 10 cm⁻¹).⁴⁵ It is possible that the two poorly resolved peaks in the photoelectron spectrum of cyclobutoxy with a spacing of 1050 ± 160 cm⁻¹ indicate that the first excited state of the cyclobutoxy radical is accessible at the photon energy used in this study. By symmetry, dissociation of the $A(^2A')$ state of cyclobutoxy would produce the first excited state of the vinoxy radical and ethylene. An examination of the energetics shows that only 0.03 eV is available to this

Table 4. Relative Energies (in eV) for the Cycloalkoxide and the Cycloalkoxy Radicals Calculated with the 6-311+G* Basis Set

	HF	MP2	QCISD	exp
AEA (c-C ₃ H ₅ O)	-0.26	1.29	1.03	1.424 ± 0.006^a
T ₀ (c-C ₃ H ₅ O)	0.23	0.55	0.43	0.741 ± 0.002^a
AEA (c-C ₄ H ₇ O)				1.7 ± 0.1^b

^a Reference 17. ^b This work.

product channel, due to the large splitting of the ground and first excited states of the vinoxy radical (1.015 eV).⁴⁰ The $N(eKE)$ and $N(E_T)$ distributions observed are not consistent with this constraint. However, nonadiabatic interactions in the $A(^2A')$ state could lead to coupling with a dissociative curve yielding ground state products. At this time it is not possible to definitively assign the structure in the photoelectron spectrum to either electronic or vibrational excitation. Future high-resolution studies with tunable laser photodetachment may assist in determining the origin of this structure.

C. Calculated Energetics. The zero-point-corrected energies calculated for the species involved in the photodetachment processes of cyclopropoxide are listed in Table 3. When compared to experimental values and observations, some of these values were in good agreement. For instance, the electron affinity of the ring-opened radical, 3-oxopropan-1-yl, was found to be very small (0.15 eV with QCISD). It is reasonable that the large amount of excess energy available after photodetachment of this anion to the ring-opened neutral radical could produce the broad feature at high electron kinetic energies (eKEs) in the photoelectron spectrum. In agreement with previous calculations, the cyclopropoxide anion was determined to be more stable than 3-oxopropan-1-ide.¹⁷ This result is consistent with the low intensity of the photodetachment signal that may be due to 3-oxopropan-1-ide. However, some of the calculated energetics deviated from the experimental observations. The previous experimental measurements of AEA and T_0 are consistently underestimated by the MP2 and QCISD methods by 10–40% (see Table 4). A thorough investigation of the basis set effects on cyclopropoxide and the cyclopropoxy radicals would be required to determine the cause of the discrepancies in the energetics. The current experiment shows that the A state of cyclopropoxy is dissociative, but the QCISD calculations predict a stable configuration with a significant (0.21 eV) barrier to dissociation. Vibrational structure is observed in the dissociative photoelectron spectrum, however, so it is probable that there is a nonadiabatic coupling of the stable potential surface to the dissociative curve. The calculation of nonadiabatic processes is complex and computationally expensive, and thus beyond the scope of this study. Finally, the dissociation of the ground-state cyclopropoxy radical is predicted to be unfavorable because of the required fission of a second C–C bond. However, the degree of spin contamination in this calculation ($\langle S^2 \rangle = 0.977$) could have been the cause of the

(41) Hoffman, R.; Woodward, R. B. *J. Am. Chem. Soc.* **1965**, *87*, 2046–2048.

(42) Burke, L. A.; Leroy, G. *Bull. Soc. Chim. Belg.* **1979**, *88*, 379–393.

(43) Bernardi, F.; Bottoni, A.; Robb, M. A.; Schlegel, H. B.; Tonachini, G. *J. Am. Chem. Soc.* **1985**, *107*, 2260–2264.

(44) Doubleday, C. *J. Am. Chem. Soc.* **1993**, *115*, 11968–11983.

(45) Ramond, T. M.; Davico, G. E.; Schwartz, R. L.; Lineberger, W. C. *J. Chem. Phys.* **2000**, *112*, 1158–1169.

anomalously high energy predicted for the transition state from the ring-opened structure to formyl and ethylene. A multireference calculation should eliminate spin contamination from higher energy states, leading to a lower barrier for this process.

Conclusion

The photodetachment processes of cyclopropoxide and cyclobutoxide have been studied at 532 nm. The ground state of the cyclopropoxy radical has both stable and dissociative components while the first excited state is dissociative. This demonstrates that photodetachment from the a'' O σ_{2p} orbital produces a more stable electronic configuration than photodetachment from the a' O σ_{2p} orbital. The correlated measurement of the translational energy of the photofragments and the electron affinities of neutral photofragments permitted the determination of the dissociation energies of cyclopropoxide, cyclobutoxide, and the corresponding radicals. The ground state of the cyclobutoxy radical has been shown to be completely dissociative. The stability of the cyclic alkoxy radicals is affected by angle and torsional strain, the hybridization of the molecular orbitals in the cycloalkyl moiety, the conjugation of the unpaired electron in the oxygen σ_{2p} orbitals with that moiety, and the orbital symmetries of the dissociation products.

Future studies of cyclopentoxide and cyclohexoxide will provide more insight into the interaction of steric forces and electronic configurations in cyclic alkoxides and alkoxy radicals.

Photodetachment of cyclopentoxide at 532 nm has been observed to produce both stable radicals and dissociation products. The greater stability of the five-membered carbon ring containing species as compared to the four-membered ring implies that the decrease in angle and torsional strain may obviate the need for conjugation of the oxygen orbitals with the ring molecular orbitals. Further investigation of these radicals will provide more information about the factors that influence stability in ring compounds.

Acknowledgment. This work was supported by the Chemistry Division of the National Science Foundation under grant CHE 97-00142. Computing resources for the theoretical work were provided by the National Partnership for Advanced Computational Infrastructure at the San Diego Supercomputer Center. R.E.C. is a Camille Dreyfus Teacher-Scholar, an Alfred P. Sloan Research Fellow, and a Packard Fellow in Science and Engineering. L.S.A. is supported by a Cota Robles Fellowship. H.J.D. acknowledges partial support from a Forschungstipendium sponsored by the Deutsche Forschungsgemeinschaft and DOE Grant DE-FG03-98ER14879. The work of Joshua Antelman on the cyclopropanol synthesis is appreciated. We thank Professor Jay S. Siegel for discussions concerning the bonding in and dissociation of the cyclopropoxy and cyclobutoxy radicals.

JA0042581